The Plant Cell, Vol. 15, 1563–1577, July 2003, www.plantcell.org © 2003 American Society of Plant Biologists

The *CUP-SHAPED COTYLEDON3* Gene Is Required for Boundary and Shoot Meristem Formation in Arabidopsis

Casper W. Vroemen,[1] Andreas P. Mordhorst, Cathy Albrecht, Mark A. C. J. Kwaaitaal, and Sacco C. de Vries

Laboratory of Molecular Biology, Department of Plant Sciences, Wageningen University, Wageningen, The Netherlands

From an enhancer trap screen for genes expressed in Arabidopsis embryos, we identified a gene expressed from the octant stage onward in the boundary between the two presumptive cotyledons and in a variety of postembryonic organ and meristem boundaries. This gene, *CUP-SHAPED COTYLEDON3* (*CUC3*), encodes a putative NAC-domain transcription factor that is homologous with CUC1 and CUC2. Analysis of a *CUC3* hypomorph and a putative *cuc3* null mutant indicates that CUC3 function is partially redundant with that of CUC1 and CUC2 in the establishment of the cotyledon boundary and the shoot meristem, thus revealing an even higher degree of redundancy in this class of genes than was thought previously. The *CUC3* expression pattern, the *cuc3* phenotypes, and *CUC3* expression in a series of shoot meristem mutants and transgenes suggest a primary role for *CUC*3 in the establishment of boundaries that contain cells with low proliferation and/or differentiation rates. The *CUC*-mediated establishment of such boundaries may be essential for the initiation of shoot meristems.

INTRODUCTION

The basic body architecture of higher plants is established during embryogenesis; however, unlike the situation in animals, almost the entire adult plant is produced postembryonically from two meristems situated at opposite ends of the embryo (Jürgens et al., 1991). The establishment of the shoot and root meristems during embryogenesis is crucial for proper plant development and thus should be tightly regulated. The developmental process through which cell groups in the embryo acquire distinct developmental fates according to their relative positions has been termed pattern formation (Jürgens et al., 1991). The final shape of the embryo is a result of the elaboration of the pattern, through the regional regulation of cellular proliferation and differentiation. For example, in dicot embryos, two cotyledonary primordia arise through increased cellular proliferation in two apical regions of the globular embryo, flanking a region of restricted proliferation. The latter region forms the boundary between the developing cotyledons and harbors the cells that contain the shoot apical meristem (SAM) (Barton and Poethig, 1993).

The elaboration of pattern through the regional regulation of cellular proliferation rates occurs not only during embryogenesis but is a recurrent mechanism during plant development. For instance, floral organs arise in concentric whorls from the floral meristem as bulges of cells separated by boundary regions with a low rate of cellular proliferation (Furner, 1996). Proliferating leaf primordia are separated from the shoot meristem by slower proliferating boundary regions (Callos and Medford, 1994), and trichomes arise through highly increased proliferation of individual leaf epidermal cells compared with the surrounding cells (Hulskamp et al., 1994). Several genes have been identified that are expressed specifically in organ or meristem boundaries. The Arabidopsis *CUP-SHAPED COTYLEDON1* (*CUC1*) (Takada et al., 2001) and *CUC2* (Aida et al., 1997) and the petunia *NO APICAL MERISTEM* (*NAM*) (Souer et al., 1996) genes are expressed in boundaries between floral organ primordia and in the boundary between the cotyledons. Mutations in these genes cause defects in the establishment of several boundaries, resulting in organ fusions. This fact suggests that boundaries are actively established and maintained. The *CUC1*, *CUC2*, and *NAM* genes all encode putative transcription factors of the NAC-domain class (Aida et al., 1997). *NAC* genes constitute a family of ~100 putative members in Arabidopsis (Arabidopsis Genome Initiative, 2000; Duval et al., 2002) and are not found in organisms other than plants.

Besides defects in the establishment of boundaries, mutations in *CUC1*, *CUC2*, and *NAM* also affect the initiation of the SAM (Souer et al., 1996; Aida et al., 1997; Takada et al., 2001), which becomes histologically and functionally distinct in the boundary between the embryonic cotyledons during normal development. *cuc1* and *cuc2* single mutants occasionally show cotyledon fusion on one side and display weak fusions of sepals and stamens in the flower. *cuc1 cuc2* double mutant seedlings have cotyledons fused on both sides and completely lack a SAM (Aida et al., 1997). Thus, *CUC1* and *CUC2* are required for boundary and SAM formation and are partially functionally redundant (Takada et al., 2001). *CUC1* and *CUC2* are required for the expression of another gene involved in SAM formation, *SHOOT MERISTEMLESS* (*STM*), which encodes a putative homeodomain transcription factor (Long et al., 1996; Aida et al., 1999). *stm* mutants also lack a SAM and display weak cotyledon fusions. *STM* is expressed in the SAM and initially also in

[1] To whom correspondence should be addressed. E-mail casper.vroemen@wur.nl; fax 31-317-48-35-84.

Article, publication date, and citation information can be found at www.plantcell.org/cgi/doi/10.1105/tpc.012203.

the boundary between the cotyledons. Thus, the *CUC*/*STM* regulatory pathway is critical for the establishment of the boundary between the cotyledons and for the initiation of the SAM (Long and Barton, 1998; Aida et al., 1999).

Once established, the SAM harbors a population of stem cells over almost the entire life cycle of the plant (Weigel and Jürgens, 2002). Shoot meristem homeostasis is maintained by a tightly controlled balance between slowly dividing stem cells in the meristem center and cells that are displaced to the periphery and undergo differentiation (reviewed by Haecker and Laux, 2001). Molecular genetic studies have identified *WUSCHEL* (*WUS*) and *CLAVATA* as components of a negative feedback loop that controls this balance (Schoof et al., 2000). *WUS* encodes a transcription factor that functions in the specification of stem cells, and *wus* mutants fail to initiate a SAM (Laux et al., 1996; Mayer et al., 1998).

In this study, we identified the *CUC3* gene, which encodes a NAC-domain protein highly similar to CUC1 and CUC2. *CUC3* was identified in an enhancer trap screen for genes involved in pattern formation during embryogenesis (Vroemen et al., 1998). *CUC3* is expressed during embryogenesis from the octant stage onward in the boundary between the presumptive cotyledons and later during development in a wide variety of plant organ and meristem boundaries. Analysis of a *cuc3* hypomorph and a putative *cuc3* null mutant shows that *CUC3* functions in the establishment of the boundary between the cotyledons and in the formation of the SAM. Moreover, *CUC3* function appears to be partially redundant with that of *CUC1* and *CUC2*. Thus, the identification of *CUC3* suggests an even greater degree of redundancy among *CUC* genes than was thought previously on the basis of *CUC1* and *CUC2*. Based on the results of *CUC3* expression analyses in shoot meristem mutants and on a transgenic background displaying ectopic shoot meristems, we propose a model in which the establishment of boundaries is a prerequisite for SAM formation.

RESULTS

Identification of Enhancer Trap Line WET368 and Molecular Cloning of *CUC3*

Line Wageningen Enhancer Trap 368 (WET368) was identified in a screen for genes expressed during Arabidopsis embryogenesis that encompassed 431 enhancer trap lines (Vroemen et al., 1998) and was selected for in-depth analysis based on its restricted expression in a region containing the embryonic SAM (Figures 1A to 1I). DNA gel blot analysis demonstrated the presence of a single *DsE* element insertion (Vroemen et al., 1998). The name WET368 refers to both the plant line carrying this enhancer trap insertion and to the actual *DsE* element inserted in this line.

Genomic DNA flanking *DsE* was amplified by thermal asymmetric interlaced PCR to isolate the gene identified by the WET368 enhancer trap and used to screen an Arabidopsis genomic library. The insert of one of the positive phages was sequenced, and BLAST (Basic Local Alignment Search Tool) searches identified two overlapping BACs, F14G6 and F15M4, spanning the phage insert. A predicted open reading frame encoding a novel NAC-domain protein of 334 amino acids was located on the overlapping region of the two BACs, 220 bp downstream of the 3′ end of the WET368 *DsE* element (Figure 2A). We named this predicted gene *NAC368*, but based on sequence similarity with the previously identified *CUC1* and *CUC2* genes (Aida et al., 1997; Takada et al., 2001) and functional data presented here, it was renamed *CUC3*. *CUC3* is located on the lower arm of chromosome 1, and the coding sequence consists of three exons of 205, 275, and 522 bp separated by two introns of 132 and 670 bp (Figure 2A). The NAC domain, which spans amino acids 22 to 171, is encoded by most of the first, the second, and the beginning of the third exons. The second exon contains a putative bipartite nuclear localization signal sequence (Kikuchi et al., 2000; Xie et al., 2000) that spans amino acids 84 to 96 and 124 to 141, suggesting that CUC3 is able to enter the nucleus (Figure 2A).

A phylogenetic tree of the NAC domains of CUC3 and previously described NAC-domain proteins revealed that CUC3 is most similar to the Arabidopsis CUC1 and CUC2 and the petunia NAM proteins (Figure 2B). The NAC domain of CUC3 shares 66, 71, and 69% amino acid sequence identity with CUC1, CUC2, and NAM, respectively (Souer et al., 1996; Aida et al., 1997; Takada et al., 2001), whereas the CUC1 and CUC2 NAC domains are 82% identical.

WET368 *β-Glucuronidase* Is Expressed in Organ and Meristem Boundaries

We examined the WET368 *β-glucuronidase* (*GUS*) expression pattern by means of which the *CUC3* gene was identified in detail. In embryos, GUS staining was detected first at the early globular stage, during which it was strongest in the apical part of the embryo (Figure 1A). We were unable to reliably detect GUS staining at earlier stages of embryogenesis. During the triangular (Figures 1B to 1D), heart (Figure 1E), and torpedo (Figure 1F) stages, *GUS* expression resolved to the center of the apical part of the embryo. From oblique (Figure 1C) and side (Figure 1D) views of triangular embryos, it appeared that WET368 *GUS* was expressed in a central stripe across the apical half of the embryo, representing the boundary between the emerging cotyledons. Between the torpedo and bending cotyledon stages, GUS staining became more prominent in the boundaries of the cotyledon margins than in the SAM region (Figure 1G). WET368 *GUS* expression remained associated with the embryo and seedling apex during further embryo and seedling development (Figures 1H to 1J). In the seedling apex, GUS staining was absent from the SAM itself and restricted to the boundaries of the cotyledon margins and the boundaries between the SAM and the cotyledons (Figure 1K).

Because WET368 *GUS* expression seemed restricted to (presumptive) boundary regions during embryo and seedling development, we next examined whether WET368 *GUS* also was expressed in other boundaries during plant development. WET368 *GUS* expression was detected in a one-cell-wide ring at the boundary between trichomes and leaf epidermis cells (Figures 1L and 1M), whereas no expression was detected in trichomes themselves (Figure 1M). This "support cell"–specific expression was not found in any other enhancer trap line in our collection (data not shown). Lateral roots were delimited at their

bases by a one-cell-wide ring of cells expressing WET368 *GUS* (Figures 1N to 1P). This expression ring appeared only after the lateral root primordium emerged from the main root. In aerial plant parts, WET368 *GUS* expression was found in the adaxial axils of secondary inflorescences (Figure 1Q) and pedicels (Figure 1R). Furthermore, *GUS* expression was observed in axillary buds (Figure 1Q). WET368 GUS staining in flower buds was detected in a ring at the bases of sepals and petals (Figure 1S). In the carpel, WET368 *GUS* expression marked the boundaries between ovule primordia (Figure 1T). Analysis of serial optical sections (data not shown) revealed that ovule primordia were encircled at their bases and separated from each other by WET368 *GUS*–expressing cells. In ovules, WET368 *GUS* expression appeared only at the approximate time of fertilization, in a ring at the boundary between the nucellus and the chalaza (Figures 1U and 1V).

In conclusion, a variety of boundaries during Arabidopsis development are marked by WET368 *GUS* expression. In general, these boundaries separate two proliferating organs or a proliferating organ or cell from its surrounding cells.

Expression of *CUC3* during Embryo Sac, Embryo, and Seedling Development

We used in situ mRNA hybridization to validate whether WET368 *GUS* expression faithfully mimicked *CUC3* expression. In the mature embryo sac, *CUC3* mRNA was detected in the two polar nuclei of the central cell (Figure 3A). The signal in the seed coat in Figures 3A to 3H also was seen in sense controls (data not shown), indicating that it does not relate to the presence of *CUC3* mRNA. No clear signal was detected in the endosperm during seed development (Figures 3B to 3L). *CUC3* mRNA was not detected in the zygote (data not shown) or in two-celled (Figure 3B) or four-celled (data not shown) embryos. During embryogenesis, *CUC3* mRNA was detected first at the octant stage, at which it was restricted to the apical half of the embryo, above the O line (Figure 3C). In early globular embryos, *CUC3* mRNA was most abundant in cells of the upper tier, although a weak signal also was detected in cells of the lower tier (Figure 3D).

From the globular stage onward, *CUC3* expression became restricted to the center of the apical part of the embryo (Figure 3E). Expression was strongest in epidermal cells, and from sagittal sections it appeared that *CUC3* expression localized to a central stripe across the apical half of the embryo (Figure 3F). This stripe represents an early manifestation of bilateral symmetry, which becomes morphologically visible only at the triangular stage, along with the appearance of the cotyledon primordia (Figure 3G). Expression in the central apical stripe continued through the triangular (Figure 3G), heart (Figure 3H), and torpedo (Figure 3I) stages of embryogenesis, remaining strongest in epidermal cells, and corresponded to the WET368 *GUS*–expressing stripe during the same stages of embryogenesis (Figures 1B to 1F). During these stages, cotyledons developed on both sides of the *CUC3*-expressing cells.

Central sections through torpedo-stage embryos showed *CUC3* expression in the presumptive SAM, extending into the boundaries between the SAM and the cotyledons (Figure 3I). Sections that were more superficial indicated that outside of the presumptive SAM, *CUC3* was expressed in a one-cell-wide boundary separating the cotyledon margins (Figure 3J). In mature embryos, *CUC3* mRNA was excluded form the SAM upon its first morphologically apparent proliferation (Figure 3K). *CUC3* expression became restricted to the boundaries between the SAM and the cotyledons (Figure 3K, arrows) and the boundaries of the cotyledon margins (Figure 3L). In both boundaries, the expression domain was one cell wide and included the epidermal and maximally one hypodermal cell layer.

Seedlings of *primordia timing* (*pt-1*) were used to examine *CUC3* expression in the seedling apex. These seedlings have an enlarged SAM (Mordhorst et al., 1998), and therefore were anticipated to give a higher spatial resolution of *CUC3* expression compared with the wild type. *CUC3* expression in *pt-1* was identical to that in the wild type, as determined by WET368 *GUS* expression (data not shown). As in mature embryos, *CUC3* expression was detected in the boundary between the SAM and the cotyledons in *pt-1* seedlings (Figure 3M). In addition, *CUC3* expression on the flank of the SAM marked the boundary between the vegetative meristem and an incipient leaf primordium (Figure 3M). Slightly later in development, proliferation of such a leaf primordium from the region enclosed by this boundary became morphologically visible (Figure 3N, arrow).

The combined WET368 *GUS* expression analysis and *CUC3* in situ hybridization data indicate that WET368 *GUS* expression (Figures 1A to 1K) faithfully mimics the *CUC3* expression pattern, although the *GUS* expression analysis has a somewhat lower cellular resolution and the in situ hybridization detects expression at a slightly earlier stage of embryogenesis. In the embryo, *CUC3* expression precedes the appearance of the morphologically visible boundary between the cotyledons. The SAM is initiated from cells within this boundary, and once initiated, its surface is isolated from the neighboring cotyledons by a *CUC3*-expressing boundary. In the seedling apex, *CUC3*-expressing cells mark the boundary between the SAM and the emerging leaf primordia. Based on this *CUC3* expression pattern and the extensive range of boundaries in adult plants marked by WET368 *GUS* expression (Figure 1), we classified *CUC3* as a boundary gene.

WET368 *GUS* Expression in *cuc* Mutants

Based on the observation that *CUC3* was expressed in boundaries, we next examined whether *CUC3* expression was affected in boundary control mutants. *cuc* mutants display variable defects in cotyledon separation and SAM formation (Aida et al., 1997). The majority of *cuc1* and *cuc2* single mutants are phenotypically normal. However, in ~0.5% of them, cotyledons are fused to a variable extent along one side, affecting the boundary of the cotyledon margins that normally expresses *CUC3*. These seedlings are called "heart-shaped seedlings" (Figure 4A). In heart-shaped *cuc2* seedlings, WET368 *GUS* expression was detected in the boundary of the SAM and in the boundary of the cotyledon margins on the nonfused side (Figures 4B and 4C), essentially as in wild-type seedlings. On the fused side, WET368 *GUS* expression was restricted to a few cells at the top of the cotyledon fusion, marking the depression that partially separates the two fused cotyledons (Figures 4B and 4D). The same WET368 *GUS* expression pattern was observed in heart-shaped *cuc1* seedlings (data not shown).

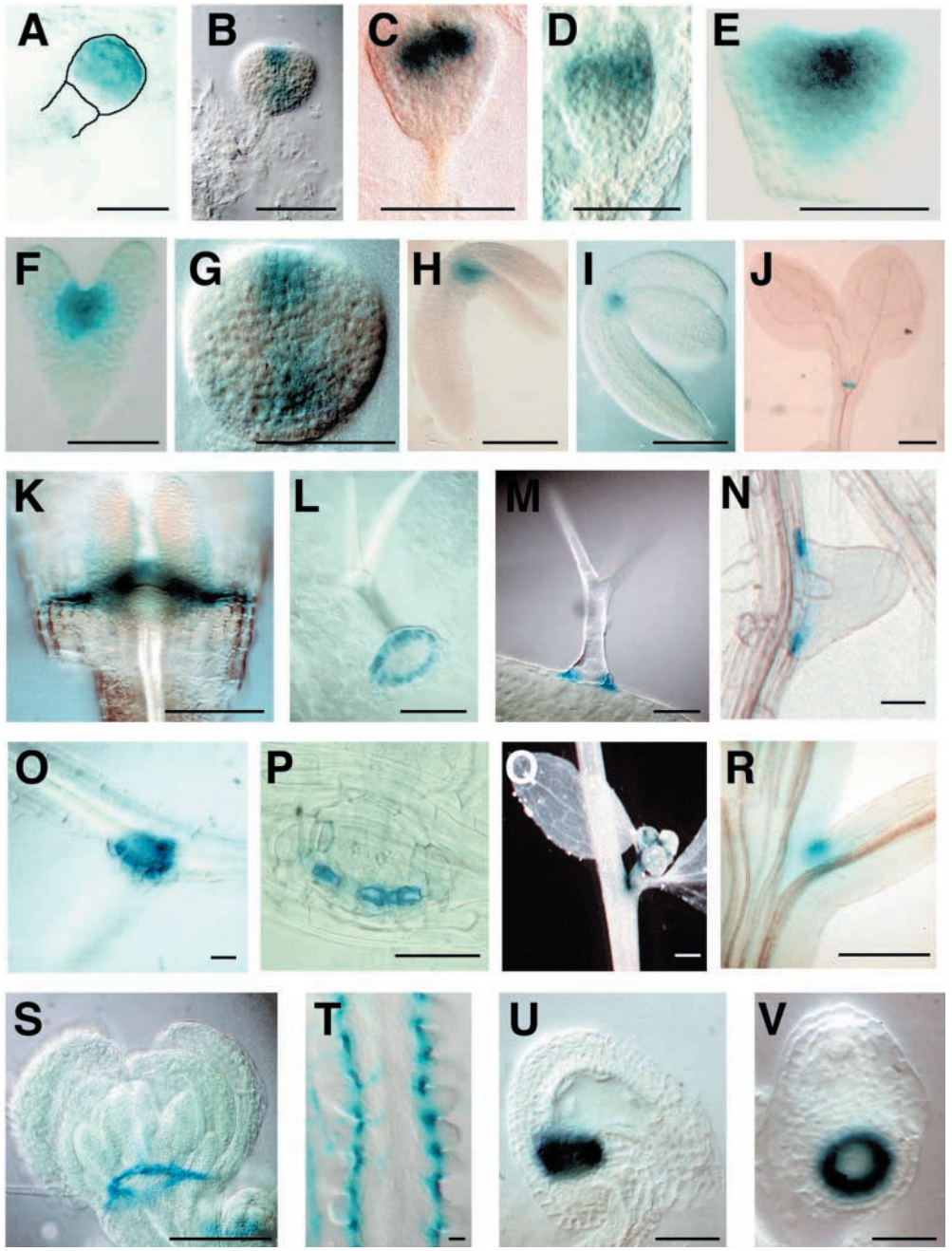

Figure 1. *GUS* Expression in WET368 Plants.

(A) Early globular embryo (the embryo and the upper part of the suspensor are outlined for clarity).
(B) Triangular-stage embryo.
(C) Triangular-stage embryo (oblique view).
(D) Triangular-stage embryo (side view).
(E) Heart-stage embryo.
(F) Torpedo-stage embryo.
(G) Bending cotyledon-stage embryo (viewed from above).
(H) Bending cotyledon-stage embryo.
(I) Mature embryo.
(J) Seedling at 5 days after germination.
(K) Seedling at 7 days after germination (side view). The frontal cotyledon has been removed to expose the SAM and the boundaries of the cotyledons.
(L) Base of a leaf trichome viewed from below.

In *cuc1 cuc2* double mutant embryos and seedlings, the cotyledons are fused along both sides, resulting in the cup-shaped cotyledon phenotype from which the mutant's name was derived (Aida et al., 1997). The upper region of almost all *cuc1 cuc2* cup-shaped cotyledons splits in two, because the cotyledons are not fused over their entire length (Figure 4E). In contrast to the single mutants, *cuc1 cuc2* double mutants always lack a SAM. Interestingly, two classes of the cup-shaped cotyledon phenotype could be distinguished among *cuc1 cuc2* seedlings carrying the WET368 *Ds* insertion (see below and Figure 5). One was the previously described cup-shaped cotyledon phenotype, in which the upper region of the cup-shaped cotyledon is split in two, as observed predominantly in *cuc1 cuc2* mutant seedlings. We called this phenotype the split cup–shaped cotyledon (s-cuc) phenotype (Figure 4E). A second, novel phenotypic class was represented by seedlings in which the upper region of the cup-shaped cotyledon was not split but entirely flat, without any sign of cotyledon separation. We called this phenotype the fully cup–shaped cotyledon (f-cuc) phenotype, which can be considered a stronger cup-shaped cotyledon phenotype than the s-cuc phenotype (Figure 4F). A similar phenotype also was reported recently in *pin-formed1* (*pin1*) *cuc1 cuc2*, *pin1 cuc1*, and *pin1 stm* mutant seedlings (Aida et al., 2002). In s-cuc seedlings, WET368 *GUS* was expressed very weakly in a few cells in the depression that partially separates the cotyledons (Figure 4G). By contrast, WET368 *GUS* expression was never observed in the upper region of fully cup–shaped cotyledons (Figure 4H). Together, these results indicate that *CUC3* expression coincides with the boundary between partially or completely separated cotyledons in *cuc* mutant seedlings. A full loss of cotyledon separation was correlated with a complete loss of WET368 *GUS* expression along the cup-shaped cotyledon rim. The observation that s-cuc seedlings displayed only weak *GUS* expression suggests that WET368 enhancer trap activation is reduced in *cuc1 cuc2* seedlings. This finding suggests that *CUC1* and *CUC2* normally stimulate the activation of the *CUC3* promoter.

Phenotypic Effects of Reduced *CUC3* Expression

We determined whether *CUC3* expression was affected by the *DsE* insertion in WET368 plants. *CUC3* mRNA levels in two individual homozygous WET368 plants, WET368A and WET368B, were compared with that of wild-type Landsberg *erecta* (L*er*) plants using reverse transcriptase–mediated (RT) PCR. Quantitative analysis showed that the *CUC3* mRNA level in homozygous WET368 plants was reduced to ~20% of the wild-type *CUC3* mRNA level (Figure 5A). As a result, CUC3 function could be reduced in homozygous WET368 plants, and the WET368 line can be considered a *CUC3* hypomorph. We named the *CUC3* hypomorph allele *cuc3-1*. No obvious mutant phenotypes were observed in hemizygous or homozygous *cuc3-1* plants. In view of the redundancy between *CUC1* and *CUC2* (Aida et al., 1997) and the similarities in sequence and expression pattern among *CUC3*, *CUC1*, and *CUC2*, we speculated that the failure to detect obvious phenotypes in *cuc3-1* plants could be attributable to redundancy between *CUC3* and the *CUC1* and *CUC2* genes. Therefore, we investigated whether the WET368 *Ds* insertion had phenotypic effects in *cuc1* and *cuc2* mutant backgrounds.

We examined the effect of hemizygous or homozygous WET368 *Ds* insertions (indicated as *cuc3-1*/+ and *cuc3-1*/*cuc3-1*) in *cuc1*, *cuc2*, and *cuc1*/+ *cuc2*/*cuc2* plants on the frequencies of heart-shaped, s-cuc, and f-cuc seedlings among their progeny. Progeny of wild-type L*er*, homozygous *cuc3-1*, *cuc1*, and *cuc2* plants, and *cuc1*/*cuc1 cuc2*/+ and *cuc1*/+ *cuc2*/*cuc2* plants were included in the analysis as references. *cuc1* plants homozygous for *cuc3-1* produced heart-shaped seedlings at a frequency of 4.4%, whereas we detected no heart-shaped seedlings among the progeny of *cuc1* plants (Figure 5B). *cuc1* plants hemizygous for *cuc3-1* produced an intermediate frequency of heart-shaped seedlings (Figure 5B). Such an intermediate frequency is expected because the progeny of *cuc1*/*cuc1 cuc3-1*/+ plants segregates for *cuc3-1* in a 1:2:1 ratio (*cuc3-1*/*cuc3-1*:*cuc3-1*/+:+/+). Likewise, *cuc2* plants homozygous for *cuc3-1* showed a 12-fold increase (0.5 to 6.2%) in the frequency of heart-shaped seedlings compared with *cuc2* plants (Figure 5B). *cuc2* plants hemizygous for *cuc3-1* exhibited an intermediate frequency of heart-shaped seedlings (Figure 5B). A similar effect of homozygous and hemizygous *cuc3-1* was seen in the *cuc1*/+ *cuc2*/*cuc2* mutant background. Here, the frequency of heart-shaped seedlings increased from 6.9 to 17.1 to 38% in the progeny of *cuc1*/+ *cuc2*/*cuc2* +/+, *cuc1*/+ *cuc2*/*cuc2 cuc3-1*/+, and *cuc1*/+ *cuc2*/*cuc2 cuc3-1*/*cuc3-1* plants, respectively (Figure 5B). These data suggest that reduced *CUC3* mRNA levels caused an increase in the percentages of heart-shaped seedlings in *cuc* mutant backgrounds.

Figure 1. (continued).

(M) Leaf trichome viewed from the side.
(N) Lateral root.
(O) and **(P)** Lateral root viewed through its base.
(Q) Axillary bud in the axil of a cauline leaf.
(R) Axil of inflorescence stem and pedicel.
(S) Flower bud.
(T) Placenta with ovule primordia.
(U) Mature ovule at approximately the time of fertilization.
(V) The same ovule as in **(U)** viewed through its chalazal end.
Bars = 40 μm in **(A)** to **(P)** and **(T)** to **(V)** and 2 mm in **(Q)** to **(S)**.

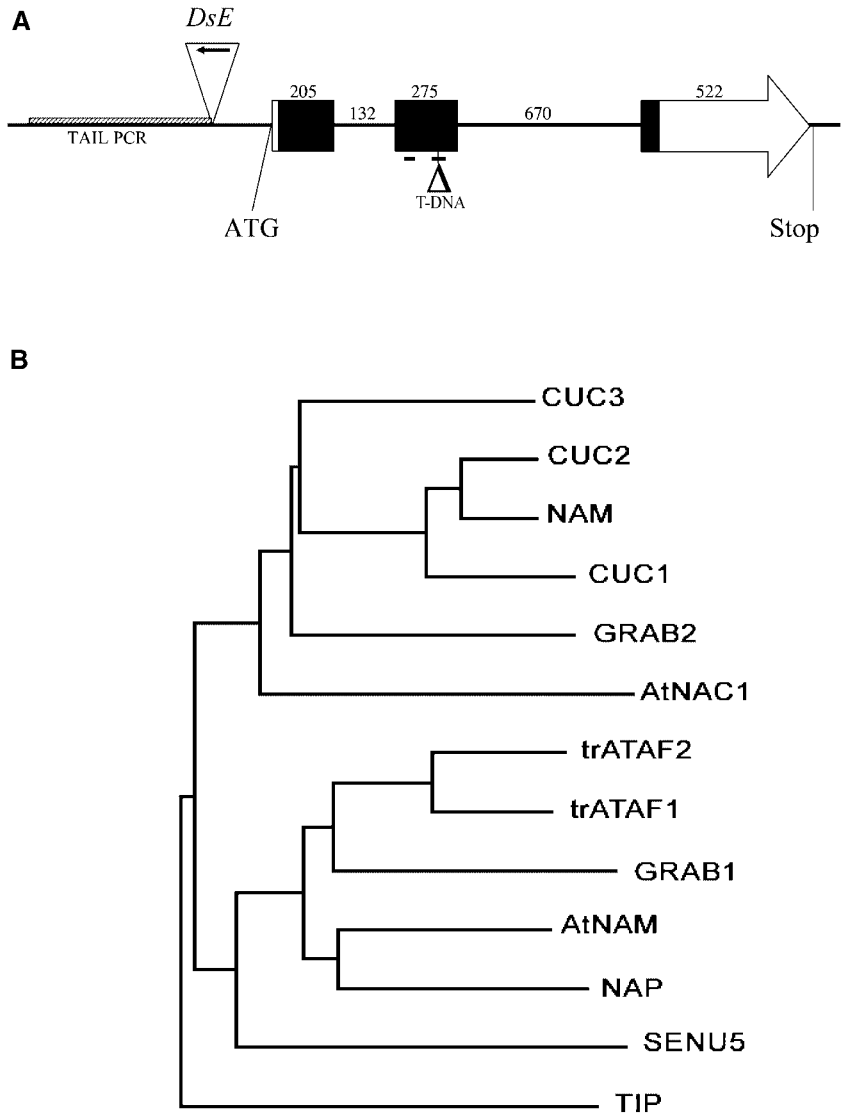

Figure 2. The *CUC3* Gene and Predicted Protein.

(A) Structure of *CUC3*. Boxes represent the open reading frame, the arrow at the end of the box at right corresponds to the C terminus of the predicted CUC3 protein, and lines indicate introns or untranslated regions. Black boxes represent nucleotides that encode the NAC domain, and numbers represent the lengths of exons and introns (in nucleotides). Lines below the second exon indicate putative bipartite nuclear localization signals. ATG and Stop indicate the start and stop codons; the triangle at left (with arrow) represents the *DsE* element in the WET368 (*cuc3-1*) line, and the arrow indicates the *GUS* gene; the shaded box represents the thermal asymmetric interlaced (TAIL) PCR product used to isolate *CUC3*; and the triangle at right indicates the Versailles T-DNA insertion in *cuc3-2*.

(B) Phylogenetic tree of the NAC domains of Arabidopsis CUC3, CUC2, CUC1, AtNAC1, ATAF1, ATAF2, AtNAM, NAP, and TIP, petunia NAM, wheat GRAB1 and GRAB2, and tomato SENU5. ATAF1 and ATAF2 are preceded by "tr" to indicate that the protein sequences were obtained by translation of mRNA sequences, leading to predicted proteins that are 60 amino acids longer than the protein sequences stored in GenBank.

To ensure that the observed phenotypic effects were caused by reduced *CUC3* expression, we studied the phenotypes of a recently identified Arabidopsis line with a T-DNA insertion in *CUC3*. This line from the Institut National de la Recherche Agronomique Versailles collection has a single T-DNA insertion (data not shown) in the second exon of *CUC3*, just before nucleotide 543 of the genomic sequence (Figure 2A). We named this *cuc3* insertion allele *cuc3-2*. No *CUC3* mRNA was detected in homozygous *cuc3-2* plants by RT-PCR (data not shown), suggesting that *cuc3-2* represents a null allele. Among the progeny of homozygous *cuc3-2*/*cuc3-2* plants, 3.1% of the seedlings were heart shaped (Figure 5B). *cuc3-2*/+ plants produced 1.1% heart-shaped seedlings, whereas wild-type Wassilewskija (Ws) plants produced no heart-shaped seedlings

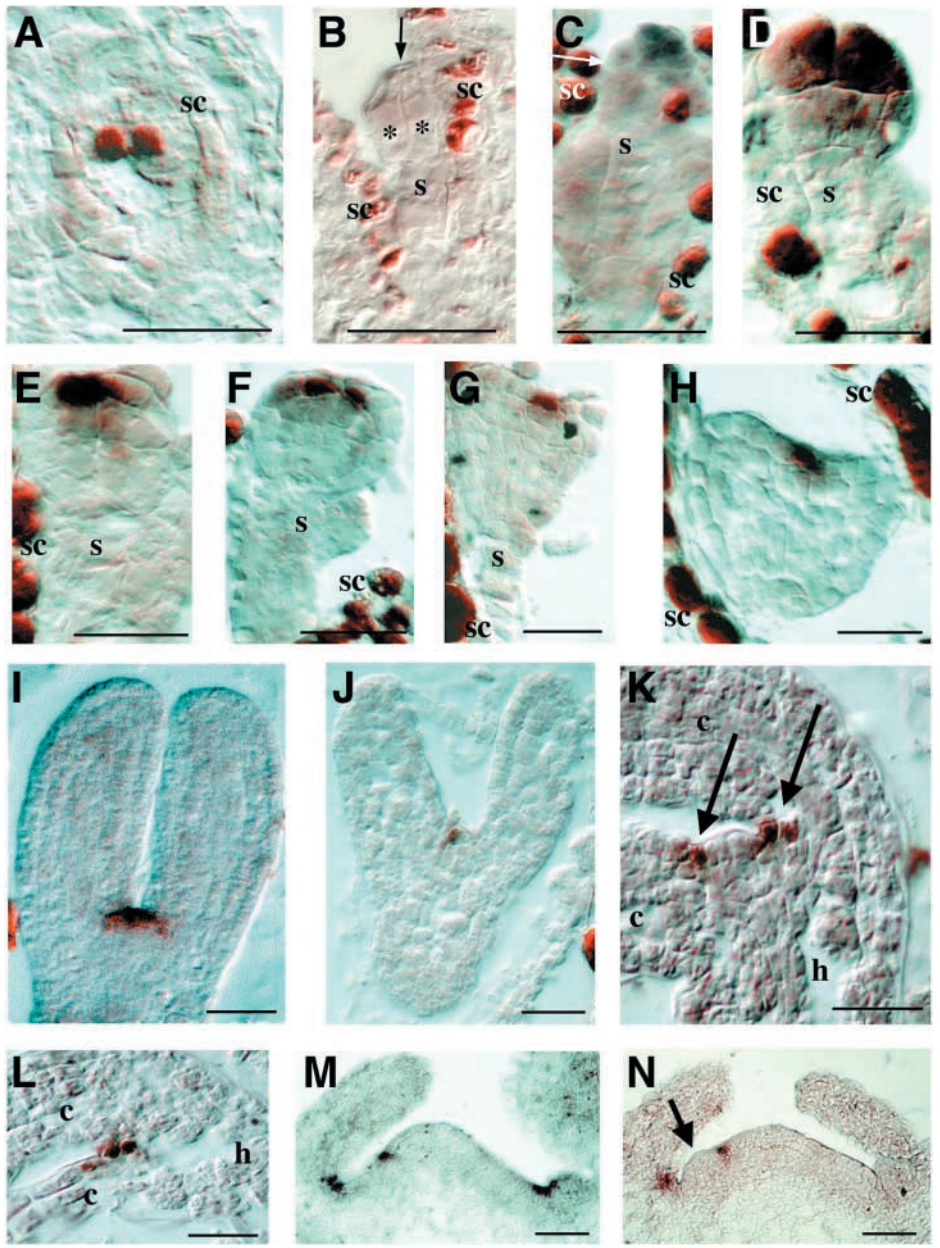

Figure 3. In Situ Localization of *CUC3* mRNA.

Sections are frontal and longitudinal unless stated otherwise.
(A) Mature embryo sac, transverse section through the polar nuclei of the central cell.
(B) Two-celled embryo (asterisks indicate the two embryo cells, and the arrow indicates the cell wall separating them).
(C) Octant-stage embryo (the arrow indicates the O line separating the upper and lower tiers).
(D) Early globular embryo.
(E) Globular embryo.
(F) Globular embryo (sagittal section).
(G) Triangular-stage embryo.
(H) Heart-stage embryo.
(I) Torpedo-stage embryo (central section through the SAM).
(J) Torpedo-stage embryo (superficial section through the boundary of the cotyledons).
(K) Mature embryo (central section through the SAM; arrows indicate the boundaries between the SAM and the cotyledons).
(L) Mature embryo (section through the boundary of the cotyledons).
(M) *pt-1* seedling apex at 5 days after germination.
(N) *pt-1* seedling apex at 5 days after germination with emerging leaf primordium (arrow).
c, cotyledon; h, hypocotyl; s, suspensor; sc, seed coat. Bars = 20 μm.

(Figure 5B). The fact that the independent *cuc3-2* insertion in *CUC3* resulted in phenotypes similar to those found for *cuc3-1* corroborates our conclusion that these phenotypes are caused by a reduction in *CUC3* expression. Notably, the *cuc3-2* mutant displayed a higher frequency of heart-shaped seedlings than the *cuc1* and *cuc2* single mutants. In addition, in contrast to the *cuc1* and *cuc2* single mutant plants, *cuc3-2/cuc3-2* and *cuc3-2/+* plants produced cup-shaped cotyledon seedlings at low frequencies (0.15 and 0.04%, respectively; Figure 5C). These cup-shaped cotyledon seedlings were similar to those found in the *cuc1 cuc2* double mutants described above with respect to the cotyledon fusion on both sides, but in contrast to these double mutants, the *cuc3-2* cup-shaped cotyledon seedlings always formed a shoot meristem (Figure 4I).

Thus, the *cuc3-2* cup-shaped cotyledon phenotype can be considered stronger than the heart-shaped phenotype but weaker than the s-cuc and f-cuc phenotypes. The higher percentage of heart-shaped seedlings and the occurrence of cup-shaped cotyledon seedlings in *cuc3-2* single mutants indicate that the *cuc3-2* mutant has a somewhat stronger phenotype than the *cuc1* and *cuc2* mutants. Thus, the contribution of *CUC3* to the establishment of the cotyledon boundary appears greater than that of *CUC1* and *CUC2*. Alternatively, because *cuc3-2* is in the Ws background and *cuc1* and *cuc2* are in L*er*, there may be greater penetrance of cotyledon boundary phenotypes in the Ws background than in L*er*.

cuc1/cuc1 cuc2/+ and *cuc1/+ cuc2/cuc2* plants produced 25% *cuc1/cuc1 cuc2/cuc2* progeny, recognizable by the cup-shaped cotyledon phenotype. The *cuc3-1* mutation did not influence the percentage of cup-shaped cotyledon seedlings among the progeny of *cuc1/+ cuc2/cuc2* plants, but the frequency of f-cuc seedlings increased from 3.4 to 23.9% in the presence of a homozygous *cuc3-1* mutation (Figure 5C). In the progeny of *cuc1/+ cuc2/cuc2 cuc3-1/+* plants, an intermediate frequency of 8.1% f-cuc seedlings was observed (Figure 5C). The observed WET368 *GUS* expression in the "rim depression" of split cup–shaped cotyledons (Figure 4G) and the increase in the relative frequency of f-cuc seedlings induced by the WET368 *Ds* insertion suggest that CUC3 function accounts for the partial cotyledon separation in *cuc1 cuc2* split cup–shaped cotyledons.

Cup-shaped cotyledon seedlings were observed not only in *cuc1 cuc2* double mutant and *cuc1 cuc2 cuc3-1* triple mutant backgrounds but also at low frequency among the progeny of *cuc2* plants homozygous or hemizygous for *cuc3-1* (Figure 5C). These *cuc2 cuc3-1* cup-shaped cotyledon seedlings always lacked a SAM, as judged by the seedling morphology and the absence of leaves and inflorescence stems later in develop-

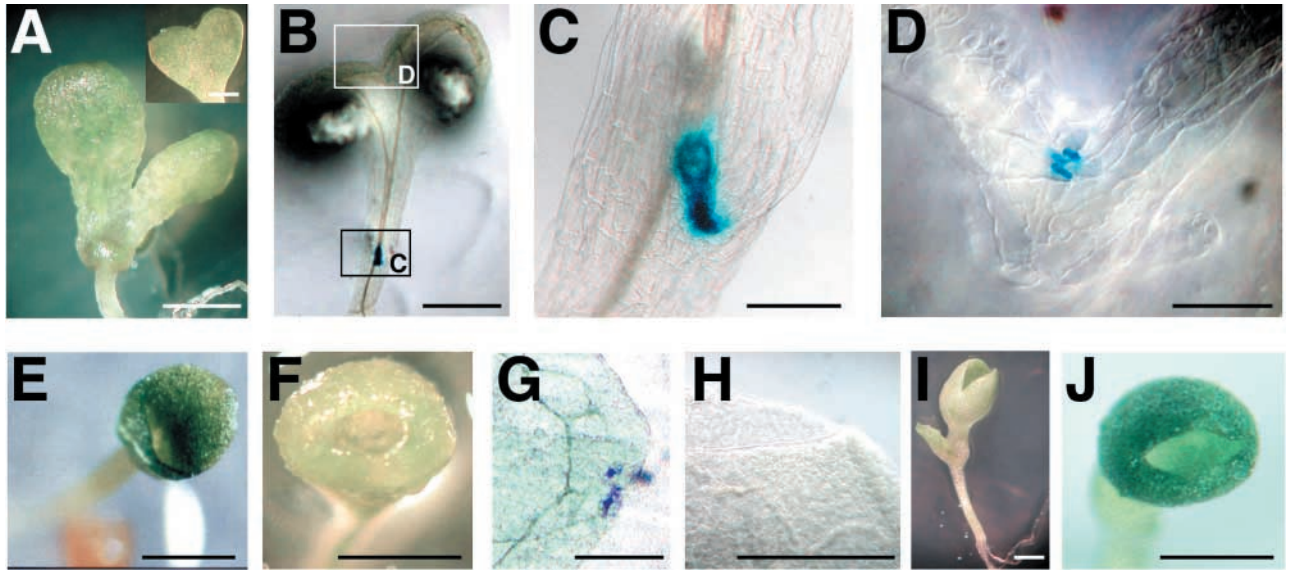

Figure 4. WET368 *GUS* Expression in WET368 *cuc* Mutant Backgrounds.

(A) Heart-shaped *cuc2* seedling. The inset shows a heart-shaped cotyledon with more extensive cotyledon fusion.
(B) Heart-shaped WET368 *cuc2* seedling after 24 h of GUS staining.
(C) Magnification of section C in **(B)** containing the SAM and the nonfused boundary of the cotyledons.
(D) Magnification of section D in **(B)** containing the top of the one-sided fusion of the cotyledons.
(E) s-cuc seedling.
(F) f-cuc seedling.
(G) Split of a *cuc1/cuc1 cuc2/cuc2* WET368/+ s-cuc seedling after 6 days of GUS staining.
(H) Flat rim of a *cuc1/cuc1 cuc2/cuc2* WET368/WET368 f-cuc seedling after 6 days of GUS staining.
(I) *cuc3-2* cup-shaped cotyledon seedling. The leaf at left originated from the SAM.
(J) Cup-shaped cotyledon seedling from the progeny of a *cuc1/+ cuc3-2/+* plant.
Bars = 1 mm in **(A)**, **(B)**, **(E)**, **(F)**, **(I)**, and **(J)** and 250 μm in **(C)**, **(D)**, **(G)**, and **(H)**.

ment. The low penetrance of cup-shaped cotyledon seedlings in the *cuc2 cuc3-1* background may be the result of the 20% residual *CUC3* expression even in homozygous *cuc3-1* plants. In contrast to *cuc2 cuc3-1*, cup-shaped cotyledon seedlings were not observed in the *cuc1 cuc3-1* background (Figure 5C). To determine whether this was the result of residual *CUC3* expression in the *cuc3-1* allele, we determined whether cup-shaped cotyledon seedlings occurred in the *cuc1 cuc3-2* background. Among the progeny of double heterozygous *cuc1/+ cuc3-2/+* plants, 6.2% of the seedlings were cup shaped (Figures 4J and 5C). This percentage represents 1/16th of the seedlings analyzed and corresponds to the expected percentage of the *cuc1/cuc1 cuc3-2/cuc3-2* genotype among the seedlings. In contrast to the cup-shaped cotyledon seedlings in the *cuc1 cuc2*, *cuc2 cuc3-1*, and *cuc1 cuc2 cuc3-1* backgrounds, *cuc1 cuc3-2* cup-shaped cotyledon seedlings formed a functional SAM. The majority of *cuc1 cuc3-2* cup-shaped cotyledons were split cup shaped (Figure 5C), in agreement with our observation that f-cuc seedlings occur mainly when the function of all three *CUC* genes is absent or strongly reduced. Besides cup-shaped cotyledon seedlings, *cuc1/+ cuc3-2/+* plants produced heart-shaped seedlings at a frequency of 4.1% (Figure 5B).

Therefore, cup-shaped cotyledon seedlings occur in the *cuc3-2* single mutant, the *cuc1 cuc2*, *cuc1 cuc3-2*, and *cuc2 cuc3-1* double mutants, and the *cuc1 cuc2 cuc3-1* triple mutant. However, only in double and triple mutant combinations containing the *cuc2* mutation (i.e., *cuc1 cuc2*, *cuc2 cuc3-1*, and *cuc1 cuc2 cuc3-1*) did these cup-shaped cotyledon seedlings lack a functional SAM. This observation suggests that

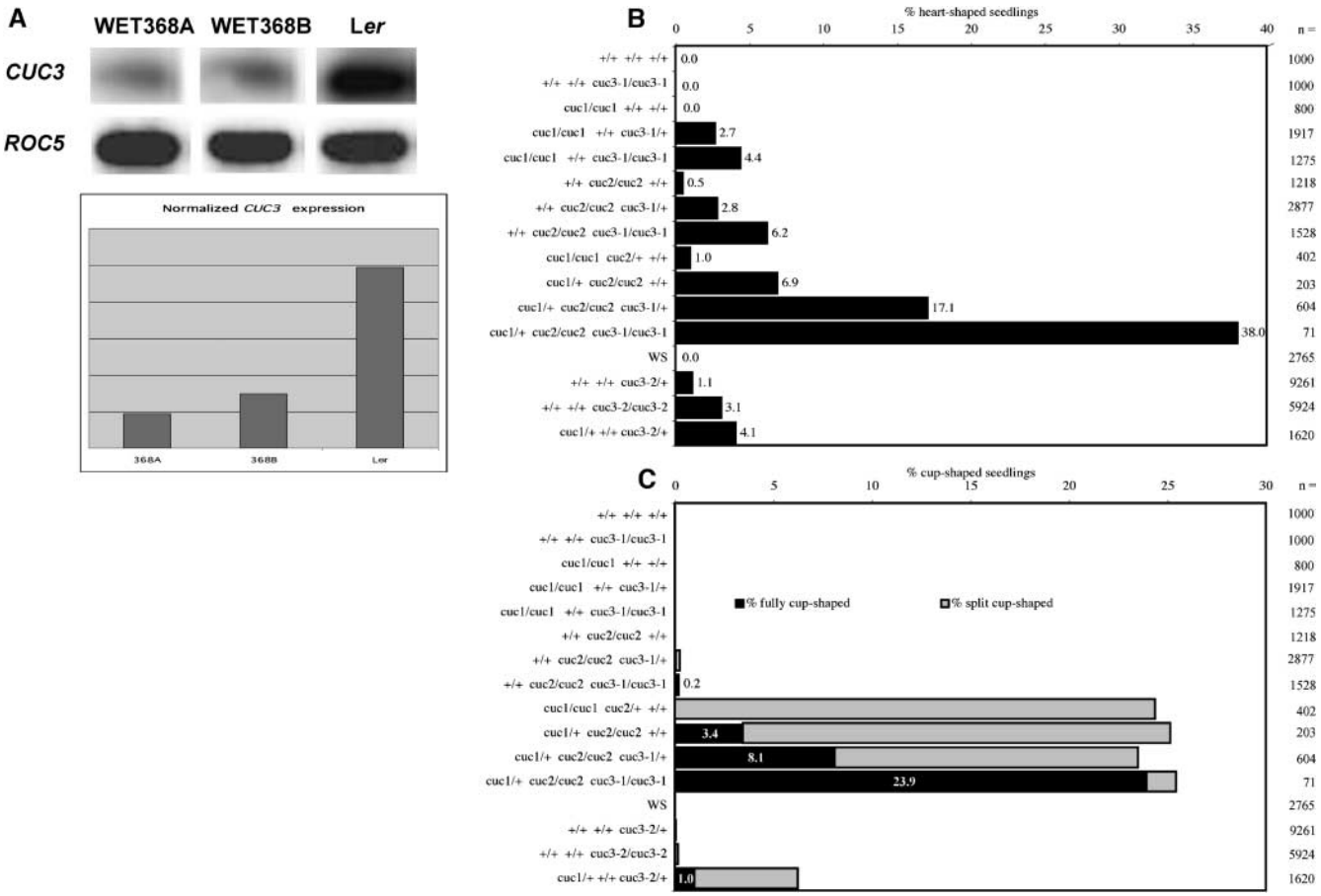

Figure 5. Phenotypic Effects of Reduced *CUC3* Expression.

(A) Semiquantitative RT-PCR of *CUC3* expression in homozygous WET368A and WET368B plants and in wild-type L*er*. *ROC5* expression was used to normalize *CUC3* expression levels.

(B) and **(C)** Relative abundance of seedling phenotypes among the progeny of plants with the indicated genotypes of *CUC1*, *CUC2*, and *CUC3*. + indicates wild-type alleles, *cuc1* and *cuc2* indicate mutant alleles, *cuc3-1* indicates the *CUC3* hypomorph allele caused by the WET368 *Ds* insertion, and *cuc3-2* indicates the *CUC3* mutant allele caused by the T-DNA insertion in exon 2. Numerals beside the bars indicate the total number of seedlings analyzed. WS, wild-type Wassilewskija.

(B) Percentages of heart-shaped seedlings.

(C) Percentages of cup-shaped cotyledon seedlings. f-cuc seedlings are shown in black, and s-cuc seedlings are shown in gray. Data labels indicate the percentages of f-cuc seedlings among the entire progeny.

among the three *cuc* mutations, only *cuc2* leads to the absence of the SAM, although only combined with mutations in *CUC1* and/or *CUC3*.

In summary, the results of our phenotypic analysis, which included two independent insertional alleles of *cuc3*, suggest a function of the *CUC3* gene in the establishment of the cotyledon boundaries and in shoot meristem formation. Its function appears to be (partially) redundant with the functions of *CUC1* and *CUC2*.

WET368 *GUS* Expression in Shoot Meristem Mutant and 35S:*KNAT1* Plants

Transgenic plants ectopically expressing the Arabidopsis homeobox gene *KNAT1* form lobed leaves, and ectopic shoot meristems occasionally develop within the boundaries, or "sinuses," between the lobes (Chuck et al., 1996). Leaf lobes in 35S:*KNAT1* plants have been proposed to result from the formation of ectopic meristem boundaries in the sinus regions (Ori et al., 2000). Because *CUC3* is expressed in meristem boundaries, we determined whether the boundaries in 35S:*KNAT1* leaves also expressed *CUC3*. Progeny plants of 35S:*KNAT1* crossed to WET368 reliably displayed the leaf phenotype seen in 35S:*KNAT1* plants. Cauline leaves of these plants displayed ectopic WET368 *GUS* expression in all sinuses. This expression preceded occasional ectopic meristem proliferation (Figure 6A). Upon meristem proliferation in a sinus, WET368 *GUS* expression resolved to the meristem boundary (Figure 6B), analogous to the situation in the proliferating embryonic SAM (Figure 3K). Thus, the appearance of morphologically visible shoot meristems in 35S:*KNAT1* leaves was preceded by the establishment of ectopic boundaries expressing *CUC3*.

We tested whether *CUC3* expression is influenced by the establishment of a functional shoot meristem by studying WET368 *GUS* expression in shoot meristem mutants. *shoot meristemless-1* (*stm-1*) seedlings are characterized by the lack of a shoot meristem (Barton and Poethig, 1993). WET368 *GUS*

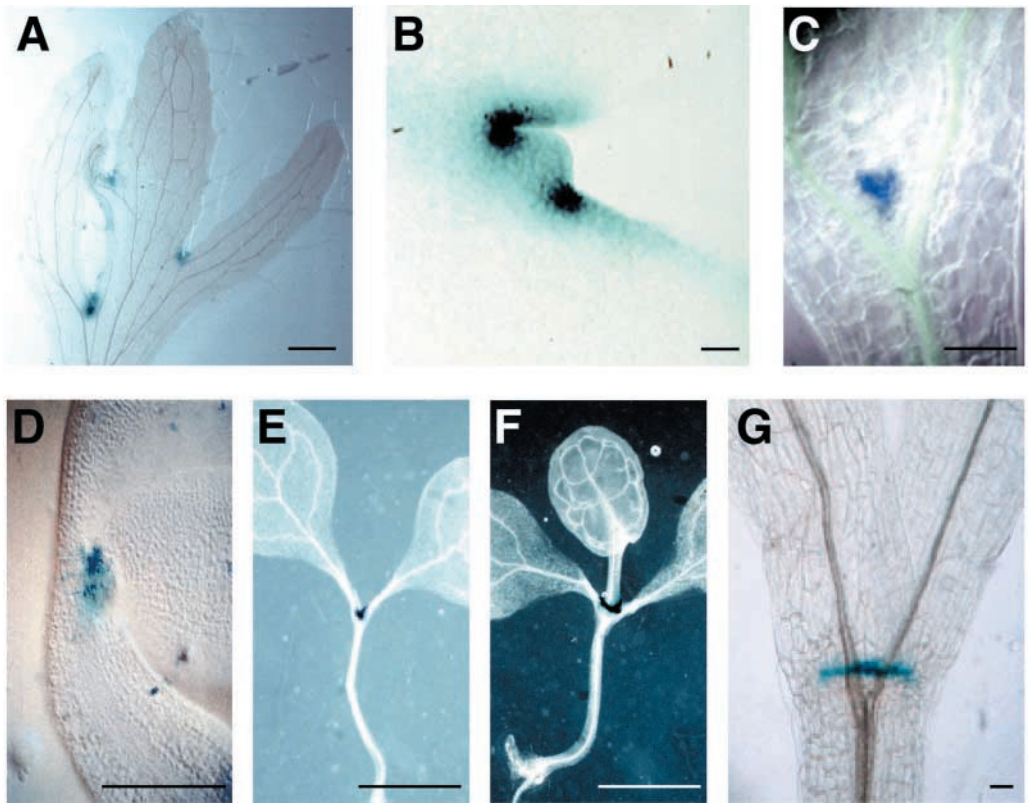

Figure 6. WET368 *GUS* Expression Patterns in Transgenic and Mutant Backgrounds.

(A) WET368 35S:*KNAT1* cauline leaf before ectopic SAM proliferation from its sinuses.
(B) Ectopic SAM in the sinus of a WET368 35S:*KNAT1* cauline leaf.
(C) WET368 *stm-1* seedling apex at 5 days after germination.
(D) Mature WET368 *zll-3* embryo.
(E) WET368 *zll-3* seedling at 5 days after germination.
(F) WET368 *zll-3* seedling at 10 days after germination with terminal leaf.
(G) WET368 *wus-1* seedling at 10 days after germination viewed from the side.
Staining times were 24 h in **(A)**, **(B)**, and **(D)** to **(F)** and 3 h in **(C)** and **(G)**. Bars = 1 mm in **(A)**, **(E)**, and **(F)** and 50 μm in **(B)** to **(D)** and **(G)**.

expression in *stm-1* seedlings localized to a narrow region that forms the boundary between the cotyledons, just above the point at which the vascular bundle splits in two (Figure 6C). Expression in the center of the boundary between the cotyledons correlates with the absence of a proliferating SAM in *stm-1*. Most embryos and seedlings of *zwille-3/pinhead* (*zll-3*) and *wuschel-1* (*wus-1*) have a dysfunctional SAM that terminates precociously with or without the formation of one or two terminal leaves in the place normally occupied by the SAM (Laux et al., 1996; Moussian et al., 1998). WET368 *GUS* expression was not affected in *zwille/pinhead* embryos (Figure 6D) or seedlings (Figure 6E), except for the persistence of *CUC3* expression in the center in the absence of meristem proliferation. Proliferation of a terminal leaf from the dysfunctional SAM in *zll-3* seedlings resulted in the exclusion of *GUS* expression from the central domain, here occupied by the terminal leaf, analogous to the situation in the wild-type seedling apex, where the central domain is occupied by the SAM (Figure 6F). The same pattern of WET368 *GUS* expression was observed in *wus* seedlings with a terminating apex (Figure 6G) or a terminal leaf (data not shown). Thus, *STM*, *ZLL*, and *WUS* functions are not required for *CUC3* expression, although the absence of a proliferating SAM in *stm*, *zll*, and *wus* correlates with persistent central *CUC3* expression. These observations indicate that *CUC3* expression is not dependent on the formation of a functional SAM.

DISCUSSION

CUC3 Encodes a Putative NAC-Domain Transcription Factor That Is Involved in Organ and Meristem Boundary Formation

The predicted CUC3 protein contains a putative bipartite nuclear localization signal within the highly conserved N-terminal NAC-domain that is characteristic of the NAC family of transcription factors (Aida et al., 1997; Duval et al., 2002) and a less conserved C-terminal domain. Phylogenetic analysis indicates that CUC3 is most similar to the Arabidopsis CUC1 and CUC2 and the petunia NAM proteins. These proteins also are most similar to CUC3 in expression pattern and function (Souer et al., 1996; Aida et al., 1999; Takada et al., 2001; this study).

During embryogenesis, the *CUC3* expression pattern largely overlaps with that of *CUC1* and *CUC2* (Aida et al., 1999; Takada et al., 2001). However, there are two main differences. First, *CUC3* is expressed earlier than both *CUC1* and *CUC2*: *CUC3* expression starts at the octant stage, whereas expression of the *CUC1* and *CUC2* genes was detected only from the globular stage onward. Second, *CUC3* expression is strongest in the epidermal cell layer, whereas *CUC1* is expressed only weakly in the epidermis and *CUC2* is not expressed in the epidermis at all. *cuc3*, *cuc1*, and *cuc2* mutations have additive phenotypic effects. Together, these results show that, although *CUC3*, *CUC1*, and *CUC2* function in the same developmental processes, they have unique expression patterns and their functions are only partially redundant.

Besides expression in embryonic boundaries, *CUC3* is expressed in a wide variety of boundaries in the seedling and adult plant, generally separating two proliferating organs or a proliferating organ or cell from its surrounding cells. None of the Arabidopsis *CUC1* (Takada et al., 2001), Arabidopsis *CUC2* (Ishida et al., 2000), and petunia *NAM* (Souer et al., 1996) genes has been reported to be expressed at the base of lateral roots and around trichomes. Thus, analysis of *CUC3* expression reveals an even broader spectrum of boundaries in plants than was thought previously. Trichomes not only differentiate differently but also grow much faster than the surrounding epidermal cells. Thus, also around trichomes, *CUC3*-expressing cells may represent a boundary that separates a highly proliferative structure from its surroundings. Interestingly, the recently identified *LATERAL ORGAN BOUNDARIES* (*LOB*) gene is expressed in a pattern similar to that of *CUC3* in the boundaries of lateral organs formed from the SAM and also in a ring of cells at the bases of lateral roots (Shuai et al., 2002). However, *LOB* expression commences later and is less localized during embryogenesis, because it was first detected in all cells of the torpedo-stage embryo.

The Identification of *CUC3* Reveals a Higher Degree of Redundancy among *CUC* Genes in Boundary and SAM Formation

cuc3-1 plants did not show any obvious phenotypes, whereas *cuc3-2* plants produced heart-shaped seedlings at low frequency. This finding indicates that the residual *CUC3* activity in *cuc3-1* plants was sufficient for normal development. The phenotypic analysis of *cuc3-2* corroborates our conclusion that the enhancement of *cuc1* and *cuc2* phenotypes by *cuc3-1* was caused by a reduction in CUC3 function. The greater frequency of heart- and cup-shaped cotyledon seedlings in the *cuc3-2* single mutant, compared with *cuc1* and *cuc2*, suggests a greater contribution of *CUC3* to the establishment of the cotyledon boundary compared with *CUC1* and *CUC2*. With respect to SAM formation, only cup-shaped cotyledon seedlings in double and triple mutant backgrounds containing the *cuc2* mutation lacked a functional shoot meristem. This finding indicates a greater contribution of *CUC2* to SAM formation compared with *CUC1* and *CUC3*. Because all *cuc2* single mutant seedlings form a functional SAM, a mutation in *CUC2* alone is not sufficient to abolish SAM formation. Only in combination with *cuc1* and/or *cuc3* does a mutation in *CUC2* lead to the absence of a functional SAM.

Our results show that *CUC3* function is partially redundant with that of *CUC1* and *CUC2*. Thus, the identification of *CUC3* suggests an even greater degree of redundancy among *CUC* genes than was thought previously on the basis of *CUC1* and *CUC2*. Bearing in mind the variety of boundaries that are marked by *CUC3* expression, *CUC3* also most likely is involved in boundary establishment and/or maintenance in adult plants, whether or not in conjunction with *CUC1* and *CUC2*. Indeed, preliminary phenotypic observations suggest a role for the *CUC3* gene in the establishment of boundaries in adult plants as well (data not shown). Our and previous studies (Aida et al., 1997, 1999; Takada et al., 2001) suggest that the extent to which the normal developmental program of boundary and SAM formation is executed is determined by the collective ac-

tivities of the *CUC1*, *CUC2*, and *CUC3* gene products. These gene products could act independently to provide threshold levels sufficient for normal development. Alternatively, in cells in which all three CUC proteins are present, the *CUC1*, *CUC2*, and *CUC3* gene products may be part of a multivalent transcription factor complex that is fully active only if all components are present or in which the reduction or absence of individual components can be partially complemented by the remaining components. This scenario is similar to the situation in the control of *Antirrhinum* floral architecture. Ternary complexes of the MADS-box transcription factors SQUAMOSA (SQUA), DEFICIENS (DEF), and GLOBOSA (GLO) have a higher target DNA binding affinity than the DEF/GLO heterodimers or SQUA/SQUA homodimers, whereas target gene activation is lost completely in the absence of all three transcription factors (Egea-Cortines et al., 1999).

Relation of *CUC3* to Other Genes Involved in Shoot Meristem Formation

Our observation that WET368 *GUS* expression does not require the activities of the *STM*, *WUS*, *CUC1*, and *CUC2* genes is in agreement with the fact that the expression of all of these genes is detected later than that of *CUC3* (Long and Barton, 1998; Mayer et al., 1998; Aida et al., 1999; Takada et al., 2001). Only *ZLL* expression precedes *CUC3* expression, but according to our results, it is not required for *CUC3* expression. Although *STM* is not required for *CUC3* expression per se, it does influence its expression level and pattern. At early stages of embryogenesis, *STM* expression overlaps with *CUC3* expression, although *STM* expression is initiated later (Long and Barton, 1998; Aida et al., 1999). By contrast, late in embryogenesis, *STM* expression appears to be complementary to that of *CUC3*, because *STM* expression resolves to the SAM while it disappears from the boundary of the cotyledon margins. In the absence of STM function, *CUC3* expression is maintained in the center of the cotyledon boundary, from which it is excluded in wild-type embryos upon the proliferation of the SAM. Thus, during normal development, either *STM* is directly involved in the downregulation of *CUC3* expression in the presumptive SAM or the downregulation of *CUC3* is an indirect consequence of *STM*-mediated SAM proliferation.

Boundaries and the Establishment of Shoot Meristems

CUC3 is expressed in a wide variety of plant organs, yet only in a restricted number of cells. What do cells that express *CUC3* have in common? *CUC3*-expressing cells are located in a boundary that separates two proliferating organs or a proliferating organ or cell from its surrounding cells. *CUC3*-expressing cells in the embryo also share this common characteristic, in that they form the boundary between the (presumptive) cotyledons. Reduction of CUC1, CUC2, and/or CUC3 function results in the incomplete establishment of this boundary. Based on these observations, we propose that *CUC3* (and *CUC1* and *CUC2*) functions primarily in the establishment and/or maintenance of boundaries at various stages of plant development. Because boundaries contain cells with restricted proliferation and/or differentiation rates, the primary function of CUC3 may be the restriction of cellular proliferation and/or differentiation.

CUC3 expression precedes SAM formation in the center of the embryo apex, and reduction of CUC3, CUC1, and CUC2 function affects not only the cotyledon boundary but also the formation of the SAM. How is the establishment of the SAM affected by the *CUC3*, *CUC1*, and *CUC2* genes? The study of transgenic plants that induce ectopic shoot meristems may provide clues to answer this question. First, plants that ectopically express the homeobox gene *KNAT1* occasionally form ectopic shoot meristems on leaf surfaces (Chuck et al., 1996). These meristems are not distributed randomly over the leaf surface but correlate strictly to ectopic boundaries that give the leaves their lobed appearance. Expression of *KNAT1* and *KNAT2* in these boundaries has given rise to the idea that the lobed-leaf phenotype results from the establishment of ectopic meristem boundaries in leaves (Ori et al., 2000). We found that *CUC3* is expressed in the ectopic leaf boundaries as well, and given its function in the establishment of the cotyledon boundary during embryo and seedling development, *CUC3* may be instrumental in the establishment of boundaries in 35S:*KNAT1* leaves. In those sinuses in which ectopic meristems are formed, *CUC3* expression precedes morphologically visible meristem formation, as it does during the establishment of the embryonic shoot meristem. Hence, *CUC3* expression and boundary formation appear to precede shoot meristem formation in 35S:*KNAT1* leaves.

Second, 35S:*CUC1* plants form lobed cotyledons. The boundaries that separate these lobes contain cells that are smaller than normal cotyledon cells (Takada et al., 2001), and ectopic shoot meristems are induced from cells within these boundaries. Thus, ectopic shoot meristems in 35S:*KNAT1* and 35S:*CUC1* backgrounds are localized to ectopic boundaries. This situation is similar to the developmental context in which the shoot meristem is established during normal embryogenesis. Our results suggest that the establishment of the boundary between the presumptive cotyledons represents one of the first patterning events that lead to shoot meristem development in the embryo. The cells within this boundary are marked by *CUC3* (and later *CUC1*, *CUC2*, and *STM*) expression (Long and Barton, 1998; Aida et al., 1999; Takada et al., 2001) and are characterized by low proliferation compared with the surrounding cells, which are destined to develop into cotyledons (Barton and Poethig, 1993). The SAM appears within the boundary, and failure to correctly establish the boundary correlates with failure to establish the SAM in plants with reduced *CUC3*, *CUC1*, *CUC2*, and/or *STM* function. Interestingly, tobacco seedlings with fused cotyledons resulting from the overexpression of phytochrome A also often lack a SAM (Emmler and Schäfer, 1997). Thus, the establishment of a boundary that contains cells with low proliferation and/or differentiation rates apparently is required for the establishment and/or maintenance of the shoot meristem.

The relatively undifferentiated cells in the boundary between the two presumptive cotyledons may provide a favorable niche for the establishment and/or maintenance of a population of stem cells. In animals, the maintenance of stem cells is dependent on the local environment, resulting in the concept of stem

cell niches (Watt and Hogan, 2000; Weigel and Jürgens, 2002). Secondary inflorescence meristems in Arabidopsis arise in the adaxial boundaries between cauline leaves and the primary stem, which also express *CUC3*. Although the *CUC* and *STM* genes, according to this idea, are required for the establishment and/or maintenance of a niche from which the SAM is initiated and maintained, they are not the only genes involved. For example, studies with the *ZWILLE*/*PINHEAD* gene (Moussian et al., 1998; Lynn et al., 1999), with members of the *YABBY* gene family (Siegfried et al., 1999), and with the *phabulosa-1d* mutant (McConnell and Barton, 1998) revealed the existence of signals from the adaxial sides of cotyledons and leaves that promote SAM initiation and/or maintenance.

How general is the proposed requirement for CUC transcription factor activity in the establishment of meristems in Arabidopsis? Although primary and secondary shoot meristems all arise from cellular regions that express *CUC3*, the root meristem presents a different case. None of the *CUC* genes is expressed in cells from which the root meristem is initiated, and reduced activity of these genes does not affect the establishment and/or maintenance of a functional root meristem (Aida et al., 1997, 1999; Takada et al., 2001; this study). A fundamental difference between the shoot and root meristems is that the former is established in the bilaterally symmetric apical part of the embryo, whereas the latter is initiated and maintained in a radially symmetric architecture (Scheres et al., 1996). In view of the possible dependence of embryonic SAM formation on the establishment of the cotyledon boundary, and thus on bilateral symmetry, it is not surprising that root meristem initiation and maintenance are governed by different regulatory networks. None of the key regulators of shoot meristem initiation described to date affects the root meristem, and vice versa (for reviews, see Scheres and Wolkenfelt, 1998; Vroemen and De Vries, 1998; Haecker and Laux, 2001). Thus, differences between meristem regulatory networks in shoots and roots may emanate from or underlie fundamental differences in local plant architecture.

METHODS

Plant Strains and Growth Conditions

The Wageningen Enhancer Trap (WET) 368 line was identified from an enhancer trap transposon-tagging screen that has been described elsewhere (Sundaresan et al., 1995; Vroemen et al., 1998). Line WET368 was obtained from a cross between starter lines *Ac*2 and *DsE*3. The wild-type and all mutant and transgenic lines were in the Landsberg *erecta* (*Ler*) background, except for the 35S:*KNAT1* line, which was in the Nossen background, and the Versailles T-DNA line *cuc3-2*, which was in the Wassilewskija background. Plants were grown in a growth chamber at 22°C with a 16-h daylength. Homozygous WET368 plants were crossed to plants heterozygous for *stm-1* or *wus-1* or homozygous for *zll-3*, *pt-1*, *cuc1*, *cuc2*, or 35S:*KNAT1*.

β-Glucuronidase Staining

β-Glucuronidase staining was performed as described previously (Vroemen et al., 1996). The duration of staining varied from 3 h to 6 days. Photographs were taken through a Nikon binocular or a Nikon Optiphot-2 microscope with Normarski optics (Tokyo, Japan). Photographs were taken on Ektachrom 16T film (Kodak) or using a Nikon Coolpix 990 digital camera.

Cloning of the *CUC3* Gene

Genomic DNA was isolated according to Bouchez et al. (1996). DNA flanking the *DsE* element in WET368 was amplified by thermal asymmetric interlaced PCR according to Parinov et al. (1999). A set of three nested primers for the 5′ end of *Ds*, Ds5-1, Ds5-2, and Ds5-3 (Grossniklaus et al., 1998), was used in combination with arbitrary primers AD1 and AD4 (Liu et al., 1995). Ten nanograms of genomic DNA was used as a substrate. After three rounds of nested amplification, reaction products were separated on a 3% (w/v) agarose gel. Secondary and tertiary reaction products were purified using the High Pure PCR Product Purification Kit (Roche, Indianapolis, IN) and cloned into the pGEM-T vector (Promega). DNA sequences were determined using an ABI 373A (Applied Biosystems, Foster City, CA) automatic sequencer using the DYEnamic ET Terminator Cycle Sequencing Kit (Amersham Pharmacia). The product obtained from reactions with AD4 was 204 bp, and from reactions with AD1 two products were obtained, one of 287 bp and one of 604 bp.

The 604-bp product was used to screen 6×10^4 clones (nine genome equivalents) of an Arabidopsis L*er* genomic library in λ FIX II (Stratagene) according to Sambrook et al. (1989). The insert of a positive phage was subcloned into pGEM-4Z (Promega) and partially sequenced. Basic Local Alignment Search Tool (BLAST) searches against The Arabidopsis Information Resource (TAIR) database (www.arabidopsis.org) identified two overlapping BAC sequences, F14G6 and F15M4. GENSCAN 1.0 (genes.mit.edu/GENSCAN.html) analysis of the DNA sequence identified a single open reading frame close to the *DsE* insertion. BLAST searches at TAIR or the National Center for Biotechnology Information identified this open reading frame as a member of the *NAC* transcription factor gene family; therefore, we named it *NAC368*. Based on the functional data presented here, the *NAC368* gene was renamed *CUP-SHAPED COTYLEDON3* (*CUC3*).

PCR primers were designed to generate nine overlapping fragments covering the entire *CUC3* gene. These primers were as follows: MKnac1 (5′-GGGTGATTTGCAGAGTGTT-3′), MKnac2 (5′-CTAGTAGCATGTGAAGAG-3′), MKnac3 (5′-CCTCGAAAACGACCATTC-3′), MKnac4 (5′-CATCAC-CTTTTGTATCATTGC-3′), MKnac5 (5′-TAACTTTTAAGAAATTTGTTCG-3′), nacf1 (5′-GAAGAAAGGAACGAGAGAGG-3′), nacr2 (5′-ACGTGTGGC-GGTGTGAATGG-3′), and nacr3 (5′-GAAGGTTCTATAAGCAAAGG-3′). PCR products were cloned into pGEM-T and sequenced, resulting in an average threefold sequence coverage of the *CUC3* gene. *CUC3* cDNA was obtained by reverse transcriptase–mediated (RT) PCR using primers nac368cDNA5 (5′-GTTATATTAAGTAAAAGATGATGC-3′) and nac368cDNA3 (5′-CAA-GGGCCAAGATTCTACAGC-3′). Sequence analyses and alignments were performed using DNASTAR (Madison, WI). Phylogenetic trees and multiple protein alignments were constructed using CLUSTAL X (1.64b).

RT-PCR Analysis

Total RNA was isolated from mixed flower buds, flowers, and siliques using TRIzol (Invitrogen, Carlsbad, CA). RT-PCR was performed according to Albrecht et al. (1998). Parallel reactions in which the RT step was omitted were used as negative controls. The constitutively expressed cyclophilin gene *ROC5* was used as a normalization control (Chou and Gasser, 1997). Linearity of PCR was determined at 30 cycles using undiluted and 4-, 16-, and 64-fold dilutions of the first-strand cDNA as templates. The primers were nacf1 and nacr3 for *CUC3* and roc5-5 (5′-TCTCTCTTCCAAATCTCC-3′) and roc5-3 (5′-AAGTCTCTCACTTTC-TCACT-3′) for *ROC5*. Hybridization signals were detected with a Storm 840 PhosphorImager and quantified using ImageQuant software (Molecular Dynamics, Sunnyvale, CA).

In Situ Hybridization

In situ hybridization was performed according to Mayer et al. (1998). Two templates were used for *CUC3* antisense and sense probes. nacex3 is a 487-bp DNA fragment from the third exon amplified from genomic DNA using MKnac1 and MKnac2 primers, and nacgen13 is a 1992-bp DNA fragment spanning the entire genomic sequence amplified from genomic DNA using MKnac4 and MKnac5 primers. Both probes gave the same qualitative and quantitative results.

Phenotypic Analyses

Homozygous WET368 plants were crossed to homozygous *cuc1* or *cuc2* plants, and F2 plants homozygous for *cuc1* or *cuc2* were selected. The *cuc1* mutation was detected by cleaved amplified polymorphic sequence analysis, and the *cuc2* mutation was detected by PCR genotyping of individual seedlings as described by Takada et al. (2001). The *cuc3-1* genotype of F2 plants was determined by plating F3 seeds on Murashige and Skoog (1962)–kanamycin plates. Seeds from *cuc1/cuc1 cuc3-1/cuc3-1*, *cuc1/cuc1 cuc3-1/+*, *cuc2/cuc2 cuc3-1/cuc3-1*, and *cuc2/cuc2 cuc3-1/+* parents were plated, and the frequency of heart-shaped, split cup–shaped, and fully cup–shaped cotyledon seedlings was determined. *cuc3-1* plants in the *cuc1 cuc2* background were obtained by crossing *cuc1/cuc1 cuc2/+* plants to *cuc2/cuc2 cuc3-1/cuc3-1* plants. F2 seeds were selected on kanamycin, and the genotypes of the *cuc1*, *cuc2*, and *cuc3-1* loci were determined. F3 seeds were analyzed phenotypically as described above. Seeds from *cuc3-2/cuc3-2* and *cuc3-2/+* parents were plated and analyzed phenotypically as described above. *cuc3-2/cuc3-2* plants were crossed to homozygous *cuc1* plants, and the progeny of the resulting double heterozygous F1 plants were analyzed phenotypically as described above.

Upon request, all novel materials described in this article will be made available in a timely manner for noncommercial research purposes.

Accession Numbers

The sequence of *CUC3* has been deposited in GenBank with accession number AF543194. The accession numbers for the two overlapping BACs are AC015450 (F14G6) and AC012394 (F15M4). The accession numbers for the proteins listed in Figure 2B are as follows: Arabidopsis CUC2 (BAA19529), CUC1 (BAB20598), AtNAC1 (AAF21437), ATAF1 (derived from X74755), ATAF2 (derived from X74756), AtNAM (AAD17314), NAP (CAA10955), and TIP (AAF87300); petunia NAM (X92205); wheat GRAB1 (CAA09371) and GRAB2 (CAA09372); and tomato SENU5 (T07182).

ACKNOWLEDGMENTS

We thank Masao Tasaka, Mitsuhiro Aida, and Ken-ichiro Hibara for a gift of *cuc1* and *cuc2* seeds and for helpful discussions; Sarah Hake for 35S:*KNAT1* seeds; and Matthieu Simon and Françoise St. Drenant for the Institut National de la Recherche Agronomique Versailles T-DNA line representing *cuc3-2*. Thanks to Rob Martienssen, Venkatesan Sundaresan, and Patty Springer for sharing the Cold Spring Harbor enhancer trap system before publication; to Achim Haecker and Thomas Laux for their help with in situ hybridization; and to Boudewijn van Veen for assistance with artwork. Kerstin Gühl, Said Hussin, Ahmed A. Ahmed, Peter Uijtdewilligen, Leonie Smeenk, Rikkert Seele, and Karin Boer are thanked for technical assistance; Megan Griffith, Henk Franssen, Ton Bisseling, Vered Raz, and Annemarie Lekkerkerker are thanked for comments on the manuscript; and Maarten Koornneef and Hans de Jong are thanked for advice concerning phenotypic analyses. This work was supported by grants from Wageningen University, the European Union Biotechnology Program (ERBIO4-CT96-0689), and the Dutch Organization for Scientific Research.

Received March 21, 2003; accepted April 24, 2003.

REFERENCES

Aida, M., Ishida, T., Fukaki, H., Fujisawa, H., and Tasaka, M. (1997). Genes involved in organ separation in Arabidopsis: An analysis of the *cup-shaped cotyledon* mutant. Plant Cell **9,** 841–857.

Aida, M., Ishida, T., and Tasaka, M. (1999). Shoot apical meristem and cotyledon formation during *Arabidopsis* embryogenesis: Interaction among the *CUP-SHAPED COTYLEDON* and *SHOOT MERISTEMLESS* genes. Development **126,** 1563–1570.

Aida, M., Vernoux, T., Furutani, M., Traas, J., and Tasaka, M. (2002). Roles of *PIN-FORMED1* and *MONOPTEROS* in pattern formation of the apical region of the *Arabidopsis* embryo. Development **129,** 3965–3974.

Albrecht, C., Geurts, R., Lapeyrie, F., and Bisseling, T. (1998). Endomycorrhizae and rhizobial Nod factors both require SYM8 to induce the expression of early nodulin genes *PsENOD5* and *PsENOD12A*. Plant J. **15,** 605–614.

Arabidopsis Genome Initiative (2000). Analysis of the genome sequence of the flowering plant *Arabidopsis thaliana*. Nature **408,** 796–815.

Barton, M.K., and Poethig, R.S. (1993). Formation of the shoot apical meristem in *Arabidopsis thaliana*: An analysis of development in the wild type and in the shoot meristemless mutant. Development **119,** 823–831.

Bouchez, D., Vittorioso, P., Courtial, B., and Camilleri, C. (1996). Kanamycin rescue: A simple technique for the recovery of T-DNA flanking sequences. Plant Mol. Biol. Rep. **14,** 115–123.

Callos, J.D., and Medford, J.I. (1994). Organ positions and pattern formation in the shoot apex. Plant J. **6,** 1–7.

Chou, I.T., and Gasser, C.S. (1997). Characterization of the cyclophilin gene family of *Arabidopsis thaliana* and phylogenetic analysis of known cyclophilin proteins. Plant Mol. Biol. **35,** 873–892.

Chuck, G., Lincoln, C., and Hake, S. (1996). KNAT1 induces lobed leaves with ectopic meristems when overexpressed in Arabidopsis. Plant Cell **8,** 1277–1289.

Duval, M., Hsieh, T.-F., Kim, S.Y., and Thomas, T.L. (2002). Molecular characterization of *AtNAM*: A member of the *Arabidopsis* NAC domain superfamily. Plant Mol. Biol. **50,** 237–248.

Egea-Cortines, M., Saedler, H., and Sommer, H. (1999). Ternary complex formation between the MADS-box proteins SQUAMOSA, DEFICIENS and GLOBOSA is involved in the control of floral architecture in *Antirrhinum majus*. EMBO J. **18,** 5370–5379.

Emmler, K., and Schäfer, E. (1997). Maternal effect on embryogenesis in tobacco overexpressing rice phytochrome A. Bot. Acta **110,** 1–8.

Furner, I.J. (1996). Cell fate in the development of the Arabidopsis flower. Plant J. **10,** 645–654.

Grossniklaus, U., Vielle-Calzada, J.P., Hoeppner, M.A., and Gagliano, W.B. (1998). Maternal control of embryogenesis by MEDEA, a Polycomb group gene in Arabidopsis. Science **280,** 446–450.

Haecker, A., and Laux, T. (2001). Cell-cell signaling in the shoot meristem. Curr. Opin. Plant Biol. **4,** 441–446.

Hulskamp, M., Misera, S., and Jürgens, G. (1994). Genetic dissection of trichome cell development in Arabidopsis. Cell **76,** 555–566.

Ishida, T., Aida, M., Takada, S., and Tasaka, M. (2000). Involvement of *CUP-SHAPED COTYLEDON* genes in gynoecium and ovule development in *Arabidopsis thaliana*. Plant Cell Physiol. **41,** 60–67.

Jürgens, G., Mayer, U., Torres-Ruiz, R.A., Berleth, T., and Miséra, S.

(1991). Genetic analysis of pattern formation in the *Arabidopsis* embryo. Development **1** (suppl.), 27–38.

Kikuchi, K., Ueguchi-Tanaka, M., Yoshida, K.T., Nagato, Y., Matsusoka, M., and Hirano, H.-Y. (2000). Molecular analysis of the *NAC* gene family in rice. Mol. Gen. Genet. **262,** 1047–1051.

Laux, T., Mayer, K.F.X., Berger, J., and Jürgens, G. (1996). The *WUSCHEL* gene is required for shoot and floral meristem integrity in *Arabidopsis*. Development **122,** 87–96.

Liu, Y.-G., Mitsukawa, N., and Oosumi, T. (1995). Efficient isolation and mapping of *Arabidopsis thaliana* T-DNA insert junctions by thermal asymmetric interlaced PCR. Plant J. **8,** 457–463.

Long, J.A., and Barton, M.K. (1998). The development of apical embryonic pattern in *Arabidopsis*. Development **125,** 3027–3035.

Long, J.A., Moan, E.I., Medford, J.I., and Barton, M.K. (1996). A member of the KNOTTED class of homeodomain proteins encoded by the *STM* gene of *Arabidopsis*. Nature **379,** 66–69.

Lynn, K., Fernandez, A., Aida, M., Sedbrook, J., Tasaka, M., Masson, P., and Barton, M.K. (1999). The *PINHEAD/ZWILLE* gene acts pleiotropically in *Arabidopsis* development and has overlapping functions with the *ARGONAUTE1* gene. Development **126,** 469–481.

Mayer, K.F.X., Schoof, H., Haecker, A., Lenhard, M., Jürgens, G., and Laux, T. (1998). Role of *WUSCHEL* in regulating stem cell fate in the *Arabidopsis* shoot meristem. Cell **95,** 805–815.

McConnell, J.R., and Barton, M.K. (1998). Leaf polarity and meristem formation in *Arabidopsis*. Development **125,** 2935–2942.

Mordhorst, A.P., Voerman, K.J., Hartog, M.V., Meijer, E.A., van Went, J., Koornneef, M., and de Vries, S.C. (1998). Somatic embryogenesis in *Arabidopsis thaliana* is facilitated by mutations in genes repressing meristematic cell divisions. Genetics **149,** 549–563.

Moussian, B., Schoof, H., Haecker, A., Jürgens, G., and Laux, T. (1998). Role of the *ZWILLE* gene in the regulation of central shoot meristem cell fate during *Arabidopsis* embryogenesis. EMBO J. **17,** 1799–1809.

Murashige, T., and Skoog, F. (1962). A revised medium for rapid growth and bioassays with tobacco tissue culture. Physiol. Plant. **15**, 473–497.

Ori, N., Eshed, Y., Chuck, G., Bowman, J.L., and Hake, S. (2000). Mechanisms that control *knox* gene expression in the *Arabidopsis* shoot. Development **127,** 5523–5532.

Parinov, S., Sevugan, M., Ye, D., Yang, W.-C., Kumaran, M., and Sundaresan, V. (1999). Analysis of flanking sequences from *Dissociation* insertion lines: A database for reverse genetics in Arabidopsis. Plant Cell **11,** 2263–2270.

Sambrook, J., Fritsch, E.F., and Maniatis, R. (1989). Molecular Cloning: A Laboratory Manual. (Cold Spring Harbor, NY: Cold Spring Harbor Laboratory Press).

Scheres, B., Mckhann, H.I., and Vandenberg, C. (1996). Roots redefined: Anatomical and genetic analysis of root development. Plant Physiol. **111,** 959–964.

Scheres, B., and Wolkenfelt, H. (1998). The *Arabidopsis* root as a model to study plant development. Plant Physiol. Biochem. **36,** 21–32.

Schoof, H., Lenhard, M., Haecker, A., Mayer, K.F.X., Jürgens, G., and Laux, T. (2000). The stem cell population of *Arabidopsis* shoot meristems is maintained by a regulatory loop between the *CLAVATA* and *WUSCHEL* genes. Cell **100,** 635–644.

Shuai, B., Reynaga-Peña, C.G., and Springer, P.S. (2002). The *LATERAL ORGAN BOUNDARIES* gene defines a novel, plant-specific gene family. Plant Physiol. **129,** 747–761.

Siegfried, K.R., Eshed, Y., Baum, S.F., Otsuga, D., Drews, G.N., and Bowman, J.L. (1999). Members of the *YABBY* family specify abaxial fate in *Arabidopsis*. Development **126,** 4117–4128.

Souer, E., van Houwelingen, A., Kloos, D., Mol, J., and Koes, R. (1996). The *No Apical Meristem* gene of petunia is required for pattern formation in embryos and flowers and is expressed at meristem and primordia boundaries. Cell **85,** 159–170.

Sundaresan, V., Springer, P., Volpe, T., Haward, S., Jones, J.D.G., Dean, C., Ma, H., and Martienssen, R. (1995). Patterns of gene action in plant development revealed by enhancer trap and gene trap transposable elements. Genes Dev. **9,** 1797–1810.

Takada, S., Hibara, K., Ishida, T., and Tasaka, M. (2001). The *CUP-SHAPED COTYLEDON1* gene of *Arabidopsis thaliana* regulates shoot apical meristem formation. Development **128,** 1127–1135.

Vroemen, C.W., Aarts, N., In der Rieden, P.M.J., Van Kammen, A., and De Vries, S.C. (1998). Identification of genes expressed during *Arabidopsis thaliana* embryogenesis using enhancer trap and gene trap *Ds*-transposons. In Cellular Integration of Signalling Pathways in Plant Development, Vol. 104, F. Lo Schiavo, R.L. Last, G. Morelli, and N.V. Raikhel, eds (Berlin: Springer-Verlag), pp. 207–232.

Vroemen, C.W., and De Vries, S.C. (1998). Flowering plant embryogenesis. In Development: Genetics, Epigenetics and Environmental Regulation, E. Russo, D. Cove, L. Edgar, R. Jaenisch, and F. Salamini, eds (Heidelberg, Germany: Springer-Verlag), pp. 121–132.

Vroemen, C.W., Langeveld, S., Mayer, U., Ripper, G., Jürgens, G., Van Kammen, A., and De Vries, S.C. (1996). Pattern formation in the Arabidopsis embryo revealed by position-specific lipid transfer protein gene expression. Plant Cell **8,** 783–791.

Watt, F.M., and Hogan, B.L.M. (2000). Out of Eden: Stem cells and their niches. Science **287,** 1427–1430.

Weigel, D., and Jürgens, G. (2002). Stem cells that make stems. Nature **415,** 751–754.

Xie, Q., Frugis, G., Colgan, D., and Chua, N.-H. (2000). *Arabidopsis* NAC1 transduces auxin signal downstream of TIR1 to promote lateral root development. Genes Dev. **14,** 3024–3036.